

人脐带间充质干细胞对 DR 大鼠视网膜神经节细胞凋亡的影响及对 p38MAPK 通路的调控作用

刘曦 孙晓萍 杨建伟 朱冬梅 王媛
郑州大学附属郑州市中心医院眼科 450000

通信作者:刘曦,Email:liu520bing@aliyun.com

【摘要】 目的 探讨人脐带间充质干细胞(hUC-MSC)对糖尿病视网膜病变(DR)模型大鼠视网膜神经节细胞(RGCs)凋亡的影响及对 p38 丝裂原活化蛋白激酶(p38MAPK)通路的调节作用。方法 取 SPF 级 8 周龄 SD 雄性大鼠 45 只,采用链脲佐菌素(STZ)腹腔注射联合高糖高脂饮食建立 DR 大鼠模型,期间每周测量大鼠空腹血糖(FBG)和体质量,采用眼底血管造影观察视网膜血管走行和渗漏情况。将 40 只建模成功大鼠按照随机数字表法随机分为模型组和 hUC-MSC 注射组,每组 20 只;另选取 20 只正常大鼠腹腔注射等量柠檬酸缓冲液并常规饲养,作为对照组。hUC-MSC 注射组玻璃体内注射 hUC-MSC,对照组和模型组玻璃体内注射等量磷酸盐缓冲液(PBS)。采用荧光金(FG)逆行示踪标记 RGCs 观察存活 RGCs 数目;采用苏木精-伊红染色观察视网膜病理学变化;采用 TUNEL 法观察 RGCs 凋亡情况;采用 Western blot 法检测视网膜组织中 B 细胞淋巴瘤/白血病-2(Bcl-2)、Bcl-2 相关 X 蛋白(Bax)、p38MAPK 和磷酸化 p38MAPK(p-p38MAPK)蛋白表达量。结果 未造模大鼠 FBG 维持在正常水平,体质量随时间逐步增长,视网膜血管走行正常,无荧光素渗漏;造模大鼠 FBG 维持在较高水平,体质量增长缓慢,且于造模 2 周开始随着病程延长,体质量逐渐下降,视网膜远端血管发生扭曲,可见毛细血管荧光素渗漏,渗漏面积较大。对照组、模型组和 hUC-MSC 注射组 RGCs 密度分别为(2 136.10±215.17)、(849.40±167.82)和(1 549.20±183.26)个/mm²,总体比较差异有统计学意义($F=115.218, P<0.01$);模型组和 hUC-MSC 注射组 RGCs 密度明显低于对照组,hUC-MSC 注射组 RGCs 密度明显高于模型组,差异均有统计学意义(均 $P<0.05$)。对照组视网膜结构清晰,层次分明,RGCs 形态完整,数目较多;模型组 RGCs 数量明显减少,出现核固缩,RGC 层变薄萎缩;hUC-MSC 注射组视网膜结构较完整,RGCs 数较模型组多。对照组、模型组和 hUC-MSC 注射组 RGCs 凋亡率分别为(2.16±1.11)%、(43.47±2.26)%和(20.75±2.18)%,总体比较差异有统计学意义($F=445.159, P<0.01$);模型组和 hUC-MSC 注射组 RGCs 凋亡率明显高于对照组,hUC-MSC 注射组 RGCs 凋亡率低于模型组,差异均有统计学意义(均 $P<0.05$)。对照组、模型组和 hUC-MSC 注射组视网膜组织 Bax、Bcl-2 和 p-p38MAPK 蛋白相对表达量总体比较差异均有统计学意义($F=30.982, 12.526, 73.158$, 均 $P<0.01$);模型组和 hUC-MSC 注射组 Bax 和 p-p38MAPK 蛋白相对表达量明显高于对照组,Bcl-2 蛋白相对表达量明显低于对照组,差异均有统计学意义(均 $P<0.05$);hUC-MSC 注射组 Bax、p-p38MAPK 蛋白相对表达量明显低于模型组,Bcl-2 蛋白相对表达量明显高于模型组,差异均有统计学意义(均 $P<0.05$)。各组 p38MAPK 蛋白相对表达量总体比较,差异无统计学意义($F=1.182, P=0.322$)。结论 hUC-MSC 玻璃体内注射可抑制 DR 模型大鼠 RGCs 凋亡,保护视网膜结构,其可能是通过抑制 p38MAPK 信号通路发挥抗细胞凋亡作用。

【关键词】 糖尿病视网膜病变;人脐带间充质干细胞;视网膜神经节细胞;凋亡

基金项目:河南省医学科技攻关计划项目(2018020799)

DOI:10.3760/cma.j.cn115989-20200804-00559

Effect of human umbilical cord derived mesenchymal stem cells on apoptosis of rat retinal ganglion cells under high glucose and on the regulation of p38MAPK pathway

Liu Xi, Sun Xiaoping, Yang Jianwei, Zhu Dongmei, Wang Yuan

Department of Ophthalmology, Zhengzhou Central Hospital Affiliated to Zhengzhou University, Zhengzhou 450000, China

Corresponding author: Liu Xi, Email: liu520bing@aliyun.com

【Abstract】 Objective To investigate the effect of human umbilical cord mesenchymal stem cells (hUC-

MSC) on the apoptosis of retinal ganglion cells (RGCs) in diabetic retinopathy (DR) model rats and on the regulation of p38 mitogen-activated protein kinase (p38MAPK) pathway. **Methods** Forty-five SPF male 8-week old SD rats were selected. The DR rat model was established by intraperitoneal injection of streptozotocin (STZ) combined with a high-sugar and high-fat diet. The fasting blood glucose (FBG) and body weight of the rats were measured every week during the high-sugar and high-fat diet, and fundus angiography was used to observe the circulation and leakage of retinal blood vessels. Forty rats with successful modeling were randomly divided into model group and hUC-MSC injection group according to the random number table method, with 20 rats in each group. Another 20 normal rats fed routinely were served as control group, and intraperitoneally injected with the same amount of citric acid buffer. The hUC-MSC injection group was injected intravitreally with hUC-MSC, and the control group and model group were injected intravitreally with the same amount of phosphate buffer saline (PBS). Fluoro gold (FG) retrograde tracer labeling RGCs was used to observe the number of survived RGCs. Hematoxylin-eosin staining was used to observe the pathological changes of retina. TUNEL method was used to observe the apoptosis of RGCs. Western blot was used to detect B cell lymphoma /leukemia-2 (Bcl-2), Bcl-2 associated X protein (Bax), p38MAPK and phosphorylated (p-) p38MAPK protein expression in retinal tissues. The use and care of the rats complied with the ARVO statement. The study protocol was approved by an Animal Ethics Committee of Zhengzhou central Hospital Affiliated to Zhengzhou University (NO. 2980316). **Results** The FBG of control rats was maintained at a normal level, and the body weight gradually increased over time, and was gradually decreased as the course of disease prolonged. The retinal blood vessels ran normally without fluorescein leakage in the control group. In the modeling group, the FBG was maintained at a high level, and the body weight increased slowly and gradually decreased with the prolongation of the disease course since the second week after modeling. The distal retinal vessels were found twisted with large area of capillary fluorescein leakage in the modeling group. The density of RGCs in the control group, model group and hUC-MSC injection group were $(2\ 136.10 \pm 215.17)$, (849.40 ± 167.82) , $(1\ 549.20 \pm 183.26)$ cells/mm², with significant overall differences ($F = 115.218, P < 0.01$). The density of RGCs in the model group and the hUC-MSC injection group were significantly lower than that of the control group, and the density of RGCs in the hUC-MSC injection group was significantly higher than that of the model group, and the differences were statistically significant (all at $P < 0.05$). The retina in the control group was with clear structure, distinct layers, and a large number of complete RGCs. The number of RGCs in the model group was significantly reduced with nuclear pyknosis, thinned and atrophied RGC layer. The retinal structure was relatively complete, and there were more RGCs in the hUC-MSC injection group than the model group. The apoptosis rates of RGCs in the control group, model group and hUC-MSC injection group were $(2.16 \pm 1.11)\%$, $(43.47 \pm 2.26)\%$, $(20.75 \pm 2.18)\%$, with significant overall difference ($F = 445.159, P < 0.01$). The apoptosis rates of RGCs in the model group and hUC-MSC injection group were significantly higher than that of the control group, and the apoptosis rate of RGCs in the hUC-MSC injection group was lower than that of the model group, and the differences were statistically significant (all at $P < 0.05$). There were statistically significant differences in the relative expression levels of Bax, Bcl-2 and p-p38MAPK proteins in the retina tissues among the three groups ($F = 30.982, 12.526, 73.158$, all at $P < 0.01$). The relative expression of Bax and p-p38MAPK protein were significantly higher, and the relative expression of Bcl-2 protein was significantly lower in the hUC-MSC injection group and the hUC-MSC injection group than those of the control group, and the differences were statistically significant (all at $P < 0.05$). The relative expression of Bax and p-p38MAPK protein was significantly lower, and the relative expression of Bcl-2 protein was significantly higher in the hUC-MSC injection group than those in the model group, and the differences were statistically significant (all at $P < 0.05$). There was no significant difference in the relative expression of p38MAPK protein among the three groups ($F = 1.182, P = 0.322$).

Conclusions Intravitreal injection of hUC-MSC can inhibit the apoptosis of RGCs in DR model rats and protect the retinal structure of rats, which may play an anti-apoptotic effect by inhibiting the p38MAPK signaling pathway.

[Key words] Diabetic retinopathy; Human umbilical cord derived mesenchymal stem cells; Retinal ganglion cells; Apoptosis

Fund program: Henan Province Medical Science and Technology Research Project (2018020799)

DOI: 10.3760/cma.j.cn115989-20200804-00559

视网膜神经节细胞 (retinal ganglion cells, RGCs) 是视网膜最早分化的神经细胞, 具有转导和加工视觉

信号的功能。长期慢性高血糖可引起 RGCs 凋亡和功能障碍, 导致视网膜形态和功能发生异常, 进而造成糖



糖尿病患者视力丧失^[1]。现有的临床治疗方法存在固有的局限性,难以完全治愈糖尿病视网膜病变(diabetic retinopathy, DR)。寻找更安全有效的治疗方法是目前 DR 研究关注的热点。间充质干细胞(mesenchymal stem cells, MSCs)是一类具有自我更新能力和多项分化潜能的干细胞,为神经再生提供有利条件,促进神经细胞再生和功能恢复^[2]。人脐带间充质干细胞(human umbilical cord derived mesenchymal stem cells, hUC-MSC)是从人脐带获取的一类 MSCs,来源广泛、取材方便、免疫原性低,可修复多种原因引起的器官损伤,其在心肌梗死、卵巢早衰等多种疾病的治疗中被广泛应用^[3-4]。已有研究证实,通过移植 hUC-MSC 对视网膜和视神经损伤具有一定修复作用^[5]。但 hUC-MSC 对 RGCs 凋亡作用机制的研究尚缺乏。本研究拟观察 hUC-MSC 玻璃体内注射对 DR 模型大鼠 RGCs 凋亡的作用,并探讨其可能的作用机制。

1 材料与方法

1.1 材料

1.1.1 实验动物 SPF 级 8 周龄 SD 雄性大鼠[SCXK(京)2016-0011,北京维通利华实验动物技术有限公司]65 只,体质量(230±20)g。大鼠于温度(20±2)℃、相对湿度(50±10)%、12 h/12 h 光暗交替的环境下适应性饲养 1 周。所有大鼠实验前全部用裂隙灯显微镜进行眼底检查,排除眼部疾病。实验动物的饲养和使用遵循美国视觉和眼科研究协会声明。本研究方案经郑州大学附属郑州市中心医院动物实验伦理委员会审核批准(批文号:20180316)。

1.1.2 主要试剂及仪器 链脲佐菌素(streptozotocin, STZ)(美国 Sigma 公司);hUC-MSC(1×10⁶ 个/管,广州赛莱拉干细胞科技股份有限公司);异硫氰酸荧光素葡聚糖(瑞典 TdB Labs AB 公司);高糖高脂饲料(江苏省协同医药生物工程有限公司);荧光金(fluoro gold, FG)(美国 Biotium 公司);TUNEL 试剂盒(瑞士 Roche 公司);免疫组化试剂盒(美国 Santa Cruz Biotechnology 公司);兔抗大鼠 B 细胞淋巴瘤/白血病-2(B cell lymphoma /leukemia-2, Bcl-2)单克隆抗体(ab182858)、Bcl-2 相关 X 蛋白(Bcl-2 associated X protein, Bax)单克隆抗体(ab32503)、p38 丝裂原活化蛋白激酶(p38 mitogen-activated protein kinase, p38MAPK)单克隆抗体(ab32142)、磷酸化 p38MAPK(phosphorylated p38 mitogen-activated protein kinase, p-p38MAPK)多克隆抗体(ab47363)、β-actin(ab8227)、辣根过氧化物酶(horseradish peroxidase, HRP)标记、山

羊抗兔 IgG(ab6721)(英国 Abcam 公司)。裂隙灯显微镜(YZ5S)、检眼镜(YZ-6E)(苏州六六视觉科技股份有限公司);脑立体定位仪(深圳瑞沃德生命科技有限公司);TOPCON50DX 型血管荧光造影机(日本 TOPCON 公司);DMi8 倒置荧光显微镜(德国 Leica 公司);PowerPac 系列电泳仪(美国 Bio-Rad 公司)。

1.2 方法

1.2.1 DR 模型的制备及分组 STZ 以 pH4.5 的柠檬酸缓冲液稀释,随机选取 45 只大鼠,按照 60 mg/kg 单次腹腔注射 STZ,诱导糖尿病大鼠模型。STZ 注射后 72 h,尾静脉采血测量大鼠血糖,连续测量 3 d,3 次血糖均≥16.7 mmol/L,视为成功建立糖尿病大鼠模型。45 只大鼠均成功建立糖尿病模型,继续饲喂高糖高脂饲料(江苏省协同医药生物工程有限公司)4 周,期间每周测一次空腹血糖(fasting blood glucose, FBG)和体质量,使其血糖维持在 16.7 mmol/L 以上,剔除实验过程中死亡及白内障大鼠 5 只,剩余 40 只大鼠。末次饲喂高糖高脂饲料后,将 50 mg/ml 异硫氰酸葡聚糖溶解于磷酸盐缓冲液(phosphate buffer saline, PBS)中后经尾静脉注入,采用眼底血管荧光造影机行眼底血管荧光造影检查,眼底出现微血管瘤或者微血管病变的大鼠视为 DR 造模成功。DR 模型大鼠按照随机数字表法分为模型组 20 只, hUC-MSC 注射组 20 只。另选取 20 只正常大鼠为对照组,腹腔注射等量柠檬酸缓冲液,饲喂正常饲料。

1.2.2 hUC-MSC 玻璃体内注射 DR 造模成功后,采用复方托吡卡胺滴眼液[参天制药(中国)有限公司]充分扩瞳后进行干预。hUC-MSC 注射组大鼠玻璃体内注射 hUC-MSC,注射剂量参照文献[6],使用微量注射器抽取 1 μl hUC-MSC(1×10⁶ 个),打散细胞,注射器于角膜缘后 1 mm 约 40°斜角进针,绕过晶状体到达视网膜中央,透过角膜和晶状体看到针尖出现进行注射,避免损伤晶状体,注射完毕后停留 30 s 后拔针。对照组和模型组大鼠注射等量 PBS。注射完毕后用红霉素眼膏(上海通用药业股份有限公司)点眼以预防炎症。各组均注射 2 次,2 次注射间隔 7 d。

1.2.3 FG 逆行示踪标记 RGCs 观察存活 RGCs 数目 末次玻璃体内注射后 7 d,每组采用随机数字表法随机取 5 只大鼠,麻醉后固定于脑立体定位仪上,颅顶备皮,分离头皮筋膜组织暴露颅骨前囟骨性标志,确定 Bregma 点,根据大鼠脑立体定位图谱确定双侧上丘及外侧膝状体,用牙科钻钻约 1 mm 直径骨孔,用 10 μl 微量注射器向 4 个骨孔注射体积分数 2% 的 FG 各 2 μl,注射完毕后,留针 5 min 再缓慢拔出针头,缝

合筋膜和皮肤。标记后 4 d, 腹腔注射麻醉大鼠, 开胸, 左心室插管用生理盐水进行灌注, 改用质量浓度 4% 多聚甲醛固定, 待四肢及尾部出现颤动、逐渐僵硬, 肝脏颜色变白时停止灌注。摘取左侧眼球, 剪除角膜、晶状体和玻璃体, 分离视网膜, 铺于载玻片上, 选取视网膜周边 4 处剪开并铺平, 50% 甘油封片, 荧光显微镜下拍照, 采用 Image Pro-Plus 软件计数 RGCs, 以每 mm^2 中的 RGCs 数量作为细胞密度。

1.2.4 苏木精-伊红染色观察视网膜形态学变化

末次玻璃体内注射后 7 d, 每组采用随机数字表法随机取 10 只大鼠过量麻醉法处死, 摘取左侧眼球, 于 4% 多聚甲醛中固定 24 h; 去除眼前节和玻璃体, 梯度浓度乙醇脱水, 二甲苯透明, 石蜡包埋, 切片连续切片, 切片厚度 4 μm , 常规苏木精-伊红染色, 中性树胶封片, 光学显微镜下观察视网膜形态变化。

1.2.5 TUNEL 染色观察 RGCs 凋亡情况

取石蜡切片, 常规脱蜡水化, 体积分数 30% H_2O_2 室温处理 10 min, PBS 冲洗; 蛋白酶 K 37 $^\circ\text{C}$ 消化 10 min, PBS 冲洗; 加入标记液于 37 $^\circ\text{C}$ 湿盒内孵育 2 h, 滴加封闭液室温封闭 30 min, 加入生物素化抗地高辛抗体于 37 $^\circ\text{C}$ 湿盒孵育 30 min, PBS 冲洗; 加入链霉亲和素-生物素-过氧化物酶复合物 (streptavidin-biotin complex, SAB) 于 37 $^\circ\text{C}$ 湿盒孵育 30 min, 二氨基联苯胺 (diaminobenzidine, DAB) 显色 5 min, 中性树胶封片, 光学显微镜下观察 RGC 层细胞凋亡情况。细胞凋亡率 = (凋亡细胞数/细胞总数) $\times 100\%$ 。

1.2.6 Western blot 法检测视网膜 Bax、Bcl-2、p38MAPK、p-p38MAPK 蛋白相对表达水平

末次玻璃体内注射后 7 d, 摘取各组剩余 5 只大鼠左侧眼球, 保存于液氮中。取液氮中保存的眼球, 剥离视网膜, 加入 RIPA 液裂解组织, 冰上孵育 30 min, 12 000 $\times g$ 4 $^\circ\text{C}$ 条件下离心 10 min, 取上清, BCA 法蛋白定量。取加样缓冲液加入蛋白样品中, 煮沸 10 min 使蛋白变性, 进行 SDS-聚丙烯酰胺凝胶电泳, 电泳结束后将蛋白转印至 PVDF 膜, 置于质量浓度 5% 脱脂奶粉中封闭 2 h; TBST 溶液洗膜, 加入 1:2 000 稀释的 Bax、Bcl-2、p38MAPK、p-p38MAPK 或 β -actin 一抗, 4 $^\circ\text{C}$ 条件下孵育过夜; TBST 溶液洗膜, 加入 1:5 000 稀释的 HRP 标记二抗, 室温下孵育 2 h; TBST 溶液洗膜, 加入 ECL 化学发光液, 曝光显影, 用 ImageJ 软件分析条带灰度值。以 β -actin 作为内参照, 计算目的蛋白与内参条带灰度比值, 作为目的蛋白相对表达量。

1.3 统计学方法

采用 SPSS 24.0 统计学软件进行统计分析。本研

究中计量资料经 W 检验呈正态分布, 以 $\text{mean} \pm \text{SD}$ 表示, 各组计量资料比较采用单因素方差分析, 两两比较采用 LSD-*t* 检验。 $P < 0.05$ 为差异有统计学意义。

2 结果

2.1 造模过程中 FBG 和体质量变化情况

实验过程中, 对照组大鼠 FBG 维持在正常水平, 体质量随时间逐步增长; 造模组大鼠 FBG 维持在较高水平, 体质量增长缓慢, 并于造模第 2 周开始, 呈现逐渐下降的趋势 (图 1)。

2.2 造模后视网膜血管走行和渗漏情况

对照组大鼠视网膜血管呈放射状排列, 分布规则, 血管走行正常, 无荧光素渗漏; 造模组大鼠视网膜远端血管发生扭曲, 形状不规则, 可见毛细血管荧光素渗漏, 渗漏面积较大 (图 2)。

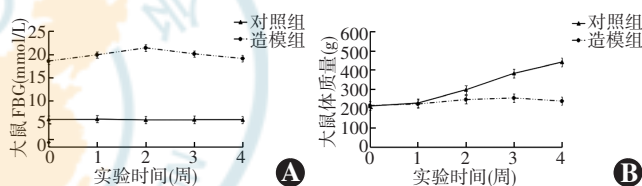


图 1 造模组和对照组大鼠 FBG 和体质量随时间变化情况 A: 各组大鼠不同时间 FBG 变化曲线 对照组大鼠 FBG 维持在正常水平; 造模组大鼠 FBG 维持在高水平 B: 各组大鼠不同时间体质量变化曲线 对照组大鼠体质量随时间平稳增长; 造模组大鼠体质量增长缓慢, 并于造模第 2 周开始逐步下降 FBG: 空腹血糖

Figure 1 Changes of FBG and body weight of rats in each group

A: Change curves of FBG The FBG of rats in the control group was maintained at a normal level, and the FBG of rats in the modeling group was maintained at a high level B: Change curves of body weight The body weight of rats in the control group was increased steadily over time, and the body weight of rats in the modeling group was increased slowly, and began to gradually decrease on the second week after modeling FBG: fasting blood glucose

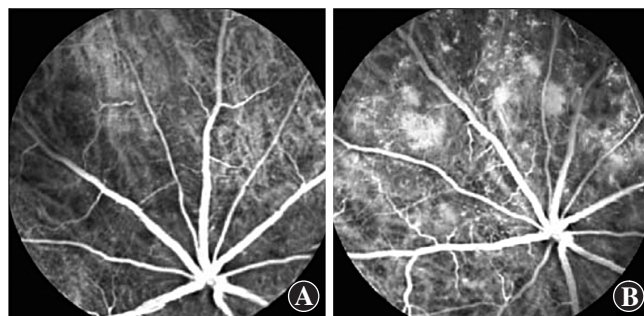


图 2 各组大鼠眼底血管荧光造影图 A: 对照组大鼠视网膜血管走行正常, 无荧光素渗漏 B: 造模组大鼠视网膜远端血管发生扭曲, 可见大面积荧光素渗漏

Figure 2 Fundus angiography images of the two groups A: The retinal blood vessels of rats in the control group run normally without fluorescein leakage B: The distal retinal vessels of rats in the modeling group were distorted and large area of fluorescein leakage was observed

2.3 各组大鼠 RGCs 存活情况变化

对照组、模型组和 hUC-MSC 注射组 FG 逆行示踪标记 RGCs 密度分别为 $(2\ 136.10 \pm 215.17)$ 、 (849.40 ± 167.82) 和 $(1\ 549.20 \pm 183.26)$ 个/ mm^2 , 各组 RGCs 密度总体比较差异有统计学意义 ($F = 115.218$, $P < 0.01$); 其中模型组和 hUC-MSC 注射组 RGCs 密度较对照组减少, 差异均有统计学意义 (均 $P < 0.05$); hUC-MSC 注射组 RGCs 密度较模型组增加, 差异有统计学意义 ($P < 0.05$) (图 3)。

2.4 各组大鼠视网膜组织病理形态学变化

对照组视网膜结构清晰, 层次分明, RGCs 形态完整, 数目较多; 模型组 RGCs 数量明显减少, 出现核固缩, RGC 层变薄萎缩; hUC-MSC 注射组视网膜结构较完整, RGCs 数目较模型组多 (图 4)。

2.5 各组大鼠 RGCs 凋亡率变化

对照组、模型组和 hUC-MSC 注射组 RGCs 凋亡率分别为 $(2.16 \pm 1.11)\%$ 、 $(43.47 \pm 2.26)\%$ 和 $(20.75 \pm 2.18)\%$, 各组 RGCs 凋亡率总体比较差异有统计学意义 ($F = 445.159$, $P < 0.01$); 其中模型组和 hUC-MSC 注射组 RGCs 凋亡率明显高于对照组, hUC-MSC 注射组 RGCs 凋亡率低于模型组, 差异均有统计学意义 (均 $P < 0.05$) (图 5)。

2.6 各组大鼠视网膜组织 Bax、Bcl-2、p38MAPK 和 p-p38MAPK 蛋

白相对表达量变化

对照组、模型组和 hUC-MSC 注射组视网膜组织 Bax、Bcl-2、p-p38MAPK 蛋白相对表达量总体比较差异有统计学意义 ($F = 30.982, 12.526, 73.158, P < 0.01$), p38MAPK 蛋白相对表达量总体比较差异无统计学意义 ($F = 1.182, P = 0.322$); 模型组和 hUC-MSC 注射组的 Bax 和 p-p38MAPK 蛋白相对表达量明显高于对照组, Bcl-2 蛋白相对表达量明显低于对照组, 差异均有统计学意义 (均 $P < 0.05$); hUC-MSC 注射组 Bax 和 p-p38MAPK 蛋白相对表达量明显低于模型组, Bcl-2 蛋白相对表达量明显高于模型组, 差异均有统计学意义 (均 $P < 0.05$)。 (图 6, 表 1)。

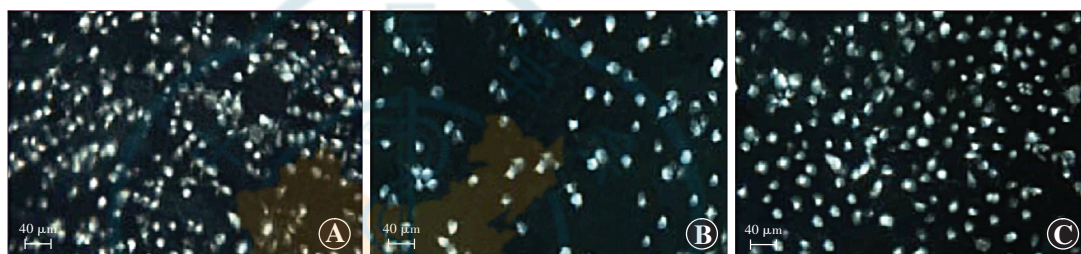


图 3 各组大鼠视网膜铺片荧光金逆行标记 RGCs 染色图 (FG $\times 200$, 标尺 = $40\ \mu\text{m}$) A: 对照组 RGCs 密度较大 B: 模型组 RGCs 密度较对照组明显降低 C: hUC-MSC 注射组 RGCs 密度较模型组升高

Figure 3 Fluoro gold retrogradely labeled RGCs staining images of retina stretched preparation in each group (FG $\times 200$, bar = $40\ \mu\text{m}$) A: The RGCs density was high in the control group B: The RGCs density in the model group was lower than that in the control group C: The RGCs density in the hUC-MSC injection group was higher than that in the model group

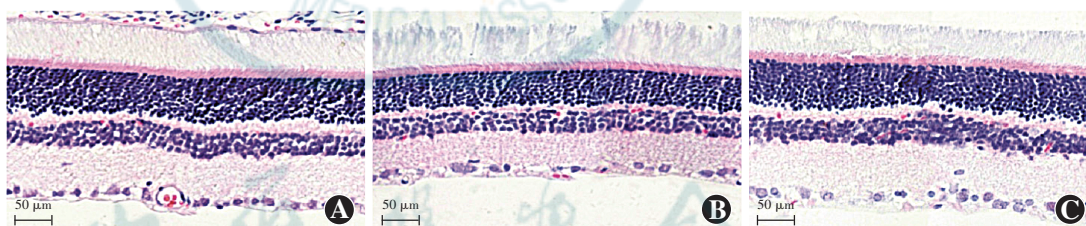


图 4 各组大鼠视网膜组织病理学染色结果 (HE $\times 400$, 标尺 = $50\ \mu\text{m}$) A: 对照组视网膜结构正常 B: 模型组视网膜 RGCs 数量较对照组减少, 出现核固缩 C: hUC-MSC 注射组视网膜结构接近对照组

Figure 4 Histopathological staining results of rat retina in each group (HE $\times 400$, bar = $50\ \mu\text{m}$) A: The retinal structure in the control group was normal B: The number of RGCs in the model group was reduced with pyknosis C: The retinal structure in the hUC-MSC injection group was similar to that in the normal group

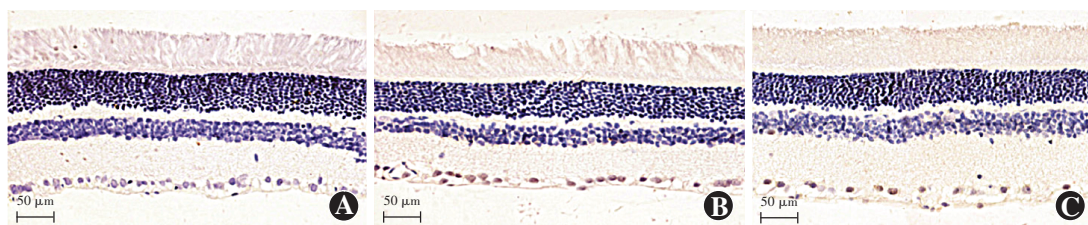


图 5 各组大鼠 RGCs 凋亡染色图 (TUNEL $\times 400$, 标尺 = $50\ \mu\text{m}$) A: 对照组未见明显 TUNEL 阳性细胞 B: 模型组 TUNEL 阳性细胞数较对照组明显增多 C: hUC-MSC 注射组 TUNEL 阳性细胞数较模型组减少

Figure 4 Apoptosis staining images of RGCs in each group (TUNEL $\times 400$, bar = $50\ \mu\text{m}$) A: No obvious TUNEL-positive cells was found in the retina of the control group B: There were more TUNEL-positive cells in the retina of model group than that of the control group C: There were fewer TUNEL-positive cells in the retina of hUC-MSC injection group than that of the model group

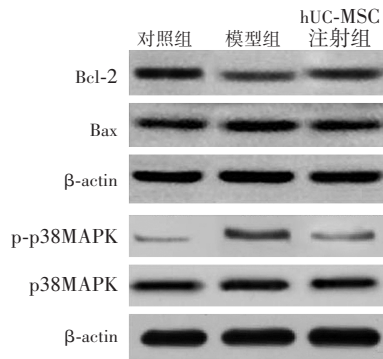


图 6 各组大鼠视网膜组织 Bax、Bcl-2、p38MAPK、p-p38MAPK 蛋白表达电泳图 模型组和 hUC-MSC 注射组 Bax 和 p-p38MAPK 蛋白表达条带较对照组增强, Bcl-2 蛋白条带较对照组减弱; hUC-MSC 注射组 Bax 和 p-p38MAPK 蛋白表达条带较模型组减弱, Bcl-2 蛋白表达条带较模型组增强, 各组 p38MAPK 蛋白表达条带强度无显著差别 Bcl-2: B 细胞淋巴瘤/白血病-2; Bax: Bcl-2 相关 X 蛋白; p38MAPK: p38 丝裂原活化蛋白激酶; p-p38MAPK: 磷酸化丝裂原活化蛋白激酶; β-actin: β-肌动蛋白; hUC-MSC: 人脐带间充质干细胞

Figure 6 Electrophoretogram of Bax, Bcl-2, p38MAPK, p-p38MAPK protein expression of retinal tissues in each group The Bax and p-p38MAPK protein expression bands were stronger and the Bcl-2 protein band was weaker in the model group and the hUC-MSC injection group than those in the control group; the Bax and p-p38MAPK protein expression bands were weaker and the Bcl-2 protein expression band was stronger in the hUC-MSC injection group than those in the model group. There was no significant difference in the intensity of the p38MAPK protein expression bands among the three groups Bcl-2: B cell lymphoma/leukemia-2; Bax: Bcl-2 associated X protein; p38MAPK: p38 mitogen-activated protein kinase; p-p38MAPK: phosphorylated-p38 mitogen-activated protein kinase; hUC-MSC: human umbilical cord derived mesenchymal stem cell

表 1 各组大鼠 Bax、Bcl-2、p38MAPK、p-p38MAPK 蛋白相对表达量比较 (mean±SD)

Table 1 Comparison of relative expression levels of Bax, Bcl-2, p38MAPK and p-p38MAPK proteins in rats among various groups (mean±SD)

组别	样本量	Bax 相对表达量	Bcl-2 相对表达量	p38MAPK 相对表达量	p-p38MAPK 相对表达量
对照组	10	0.78±0.08	0.81±0.09	0.53±0.05	0.28±0.04
模型组	10	1.12±0.11 ^a	0.63±0.07 ^a	0.56±0.06	0.51±0.05 ^a
hUC-MSC 注射组	10	0.91±0.10 ^{ab}	0.72±0.08 ^{ab}	0.57±0.07	0.35±0.04 ^{ab}
F 值		30.982	12.526	1.182	73.158
P 值		<0.001	<0.001	0.322	<0.001

注: 与对照组比较, ^a $P < 0.05$; 与模型组比较, ^b $P < 0.05$ (单因素方差分析, LSD-*t* 检验) hUC-MSC: 人脐带间充质干细胞; Bax: Bcl-2 相关 X 蛋白; Bcl-2: B 细胞淋巴瘤/白血病-2; p38MAPK: p38 丝裂原活化蛋白激酶; p-p38MAPK: 磷酸化丝裂原活化蛋白激酶

Note: Compared with the control group, ^a $P < 0.05$; compared with the model group, ^b $P < 0.05$ (One-way ANOVA, LSD-*t* test) hUC-MSC: human umbilical cord derived mesenchymal stem cell; Bax: Bcl-2 associated X protein; Bcl-2: B cell lymphoma / leukemia-2; p38MAPK: p38 mitogen-activated protein kinase; p-p38MAPK: phosphorylated-p38 mitogen-activated protein kinase

3 讨论

DR 与糖尿病病程密切相关, 病程越长 DR 发病率越高。高血糖可引起细胞内渗透压升高、电解质代谢紊乱, 破坏细胞结构的完整性, 还可结合蛋白质、脂质等物质, 引起细胞损伤和凋亡, 导致视网膜微血管病变和神经元功能受损^[7-8]。细胞凋亡在 DR 发生和发展过程中起重要作用, DR 患者早期可表现出 RGCs 凋亡现象, 而 RGCs 细胞凋亡是引起视力下降的主要原因, 抑制高糖诱导 RGCs 细胞凋亡对保护糖尿病患者视力具有重要意义^[9-10]。张惟等^[11]研究证实, hUC-MSC 能明显修复 DR 大鼠视网膜损伤, 对 DR 视神经损伤具有一定治疗作用。另有研究显示, 抑制 p38MAPK 通路, 能够增强 hUC-MSC 的组织修复能力^[12]。鉴于 hUC-MSC 对神经损伤具有保护作用且与 p38MAPK 信号通路有关, 本研究探讨玻璃体内注射 hUC-MSCs 对 DR 模型大鼠 RGCs 凋亡的抑制作用及对 p38MAPK 信号通路的调控作用。

MSCs 是治疗多种疾病的细胞来源, 可分化为神经元细胞, 还可分泌神经营养因子, 促进神经细胞存活, 对视网膜退行性病变有良好的效果, 对视神经损伤患者视力、闪光型视觉诱发电位均有明显改善效果^[13-14]。hUC-MSC 是 MSCs 主要来源之一, 具有干细胞的一般特点, 可向损伤部位定向迁移, 修复组织损伤。已有研究显示 hUC-MSC 分化为神经元样细胞, 并能表达神经细胞标志物, 其诱导分化的神经干细胞能增加糖尿病模型大鼠视网膜 RGCs 数量, 表明 hUC-MSC 具有一定的神经保护作用^[15]。本研究结果显示, 参与造模的大鼠 FBG 维持在高水平, 体质量逐渐下降, 且视网膜远端血管发生扭曲, 毛细血管出现荧光素渗漏, 表明 DR 模型建立成功。在使用 hUC-MSC 注射后, RGCs 数量较模型组明显增多, 细胞凋亡率较模型组明显降低, 视网膜病理学形态得到显著改善, 提示 hUC-MSC 可减少 RGCs 凋亡, 减轻视网膜病理损伤。Yao 等^[16]研究显示, hUC-MSC 可减轻氧化应激反应, 进而防止肝脏缺血-再灌注损伤引起的肝细胞凋亡。Liu 等^[17]研究表明, hUC-MSC 外泌体可抑制 H9C2 细胞凋亡。以上研究均提示 hUC-MSC 在抑制细胞凋亡方面具有重要作用。基于以上研究, 推测 hUC-MSC 可抑制 RGCs 凋亡, 对 DR 大鼠视网膜结构有一定保护作用。

Bcl-2 是常见凋亡抑制基因, Bax 是 Bcl-2

家族相关成员之一,具有促进细胞凋亡的作用。高糖可激活 RGCs 内 MAPK 相关通路,导致 Bax 和 Bcl-2 表达异常,引起细胞内线粒体损伤,降低 RGCs 活性,进而诱导细胞凋亡^[18]。MAPK 信号通路广泛存在于各种细胞中,参与细胞增生、分化和凋亡等生物学过程,与 DR 发生发展过程密切相关^[19]。p38MAPK 属于 MAPK 经典途径,是多种细胞信息传导的共同通路,在应激及细胞因子等因素刺激下,p38MAPK 被激活或过度表达,形成活性形式 p-p38MAPK,继而诱导 Bax 蛋白激活并转移到线粒体外膜,促进脑组织神经元细胞及静脉内皮细胞凋亡^[20-21]。刘高虹等^[22]研究表明,高糖可诱导肾小管上皮细胞 p-p38MAPK 表达升高,进而诱导上皮细胞 Bax 蛋白表达增加和 Bcl-2 蛋白表达减少,参与诱导细胞凋亡。本研究结果显示,模型组视网膜组织中 p-p38MAPK 蛋白和 Bax 相对表达量较对照组明显升高,Bcl-2 蛋白相对表达量较对照组降低,推测视网膜组织 p38MAPK 信号通路在 DR 过程中被激活,并参与 RGCs 凋亡过程;hUC-MSC 注射组 p-p38MAPK 和 Bax 蛋白相对表达量明显低于模型组,且 Bcl-2 蛋白相对表达量高于模型组,推测 hUC-MSC 可能通过 p38MAPK 信号通路抑制 RGCs 凋亡。

综上所述,本研究结果证实,hUC-MSC 对 DR 大鼠视网膜损伤具有一定保护作用,可能通过阻断 p38MAPK 信号通路来抑制 RGCs 凋亡,改善视网膜病理损伤,从而延缓 DR 进展,为临床治疗 DR 提供一定理论参考。但本研究仅为在体动物水平研究,尚缺乏安全性研究和离体细胞水平实验研究结果,其安全性和有效性有待进一步验证。此外,本研究中仅使用单一剂量进行干预,其是否可作为最适剂量,仍需进行剂量实验以验证效果。

利益冲突 所有作者均声明不存在任何利益冲突

参考文献

- [1] Tian M, Liu S, Liu L, et al. Correlations of the severity of diabetic retinopathy with EPO, caspase-3 expression and oxidative stress [J]. *Eur Rev Med Pharmacol Sci*, 2019, 23 (22) : 9707-9713. DOI: 10.26355/eurrev_201911_19532.
- [2] 栾双宇,曾亮,陈宾,等.骨髓间充质干细胞调节大鼠视神经损伤后小胶质细胞的活化[J]. *中国组织工程研究*, 2020, 24 (25) : 3937-3942. DOI: 10.3969/j.issn.2095-4344.2101. Luan SY, Zeng L, Chen B, et al. Effect of bone marrow mesenchymal stem cells on microglial activation after optic nerve injury in rats [J]. *J Clin Rehabil Tis Eng Res*, 2020, 24 (25) : 3937-3942. DOI: 10.3969/j.issn.2095-4344.2101.
- [3] Zhao L, Cheng G, Choksi K, et al. Transplantation of human umbilical cord blood-derived cellular fraction improves left ventricular function and remodeling after myocardial ischemia/reperfusion [J]. *Circ Res*, 2019, 125 (8) : 759-772. DOI: 10.1161/CIRCRESAHA.119.315216.
- [4] Lu X, Cui J, Cui L, et al. The effects of human umbilical cord-derived mesenchymal stem cell transplantation on endometrial receptivity are associated with Th1/Th2 balance change and uNK cell expression of uterine in autoimmune premature ovarian failure mice [J/OL]. *Stem Cell Res Ther*, 2019, 10 (1) : 214 [2021-05-01]. <http://www.ncbi.nlm.nih.gov/pubmed/31331391>. DOI: 10.1186/s13287-019-1313-y.
- [5] Millán-Rivero JE, Nadal-Nicolás FM, García-Bernal D, et al. Human Wharton's jelly mesenchymal stem cells protect axotomized rat retinal ganglion cells via secretion of anti-inflammatory and neurotrophic factors [J/OL]. *Sci Rep*, 2018, 8 (1) : 16299 [2021-05-01]. <http://www.ncbi.nlm.nih.gov/pubmed/30389962>. DOI: 10.1038/s41598-018-34527-z.
- [6] 王帅,董洪选,陈丹莹,等.人脐带间充质干细胞移植联合小剂量超短波对大鼠脊髓损伤星形胶质细胞形成的影响[J]. *中国康复医学杂志*, 2021, 36 (6) : 649-656. DOI: 10.3969/j.issn.1001-1242.2021.06.002. Wang S, Dong HX, Chen DY, et al. Effects of human umbilical cord mesenchymal stem cell transplantation combined with low dose ultra-short wave on the formation of astrocytes after spinal cord injury in rats [J]. *Chin J Rehabil Med*, 2021, 36 (6) : 649-656. DOI: 10.3969/j.issn.1001-1242.2021.06.002.
- [7] Wang H, Tao Y. Choroidal structural changes correlate with severity of diabetic retinopathy in diabetes mellitus [J/OL]. *BMC Ophthalmol*, 2019, 19 (1) : 186 [2021-05-01]. <http://www.ncbi.nlm.nih.gov/pubmed/31419954>. DOI: 10.1186/s12886-019-1189-8.
- [8] Mu PW, Tang XX, Tan Y, et al. Effect of basal insulin supplement therapy on diabetic retinopathy in short-duration type 2 diabetes: a one-year randomized parallel-group trial [J]. *J Diabetes*, 2019, 11 (12) : 949-957. DOI: 10.1111/1753-0407.12928.
- [9] Zhang J, Cui C, Xu H. Downregulation of miR-145-5p elevates retinal ganglion cell survival to delay diabetic retinopathy progress by targeting FGF5 [J]. *Biosci Biotechnol Biochem*, 2019, 83 (9) : 1655-1662. DOI: 10.1080/09168451.2019.1630251.
- [10] Ye Q, Lin YN, Xie MS, et al. Effects of etanercept on the apoptosis of ganglion cells and expression of Fas, TNF- α , caspase-8 in the retina of diabetic rats [J]. *Int J Ophthalmol*, 2019, 12 (7) : 1083-1088. DOI: 10.18240/ijo.2019.07.05.
- [11] 张惟,段红涛,陈松,等. PEDF 基因修饰人脐带间充质干细胞对糖尿病大鼠视网膜的保护作用 [J]. *中华眼科杂志*, 2017, 53 (7) : 540-547. DOI: 10.3760/cma.j.issn.0412-4081.2017.07.013. Zhang W, Duan HT, Chen S, et al. The protective effect of pigment epithelial-derived factor modified human umbilical cord mesenchymal stem cells on rats with diabetic retinopathy [J]. *Chin J Ophthalmol*, 2017, 53 (7) : 540-547. DOI: 10.3760/cma.j.issn.0412-4081.2017.07.013.
- [12] 方明霞,董艺超,成子安,等. P38 MAPK 通路抑制剂对 UC-MSC 功能的影响 [J]. *中国计划生育学杂志*, 2021, 29 (5) : 866-869, 1077-1079. DOI: 10.3969/j.issn.1004-8189.2021.05.003. Fang MX, Dong YC, Cheng ZA, et al. Effect of P38 MAPK pathway inhibitor on the function of UC-MSC [J]. *Chin J Fam Plan*, 2021, 29 (5) : 866-869, 1077-1079. DOI: 10.3969/j.issn.1004-8189.2021.05.003.
- [13] Ji S, Lin S, Chen J, et al. Neuroprotection of transplanting human umbilical cord mesenchymal stem cells in a microbead induced ocular hypertension rat model [J]. *Curr Eye Res*, 2018, 43 (6) : 810-820. DOI: 10.1080/02713683.2018.1440604.
- [14] Jha KA, Pentecost M, Lenin R, et al. TSG-6 in conditioned media from adipose mesenchymal stem cells protects against visual deficits in mild traumatic brain injury model through neurovascular modulation [J/OL]. *Stem Cell Res Ther*, 2019, 10 (1) : 318 [2021-05-04]. <http://www.ncbi.nlm.nih.gov/pubmed/31690344>. DOI: 10.1186/s13287-019-1436-1.
- [15] 张鹏,赵宗茂,李建华,等.单唾液酸四己糖神经节苷脂最佳质量浓度诱导人脐带间充质干细胞向神经元样细胞的分化 [J]. *中国组织工程研究*, 2018, 22 (13) : 2039-2044. DOI: 10.3969/j.issn.2095-4344.0490. Zhang P, Zhao ZM, Li JH, et al. Monosialotetrahexosyl ganglioside at an optimal concentration: inducing neuron-like differentiation of human

umbilical cord mesenchymal stem cells [J]. J Clin Rehabil Tis Eng Res, 2018, 22 (13) : 2039-2044. DOI: 10. 3969/j. issn. 2095-4344. 0490.

[16] Yao J, Zheng J, Cai J, et al. Extracellular vesicles derived from human umbilical cord mesenchymal stem cells alleviate rat hepatic ischemia-reperfusion injury by suppressing oxidative stress and neutrophil inflammatory response [J]. FASEB J, 2019, 33 (2) : 1695-1710. DOI: 10. 1096/fj. 201800131RR.

[17] Liu H, Sun X, Gong X, et al. Human umbilical cord mesenchymal stem cells derived exosomes exert antiapoptosis effect via activating PI3K/Akt/mTOR pathway on H9C2 cells [J/OL]. J Cell Biochem, 2019, 120(9) : 14455-14464 [2021-05-10]. http://www. ncbi. nlm. nih. gov/pubmed/30989714. DOI: 10. 1002/jcb. 28705.

[18] 杨慧慧, 阚全娥, 于璐, 等. 小干扰 RNA-TLR9 对高糖下大鼠视网膜神经节细胞凋亡的抑制作用及其机制 [J]. 中华实验眼科杂志, 2020, 38 (1) : 38-44. DOI: 10. 3760/cma. j. issn. 2095-0160. 2019. 10. 008.

Yang HH, Kan QE, Yu L, et al. Inhibitory effect of small interfering RNA-TLR9 on high glucose-induced retinal ganglion cell apoptosis [J]. Chin J Exp Ophthalmol, 2020, 38 (1) : 38-44. DOI: 10. 3760/cma. j. issn. 2095-0160. 2019. 10. 008. 1.

[19] 崔春梅, 李月华, 刘颖, 等. 抑制免疫抑制因子 COX-2 对视网膜神经节细胞凋亡的影响及 p38MAPK 信号的调控作用 [J]. 中国免疫学杂志, 2019, 35 (2) : 156-160. DOI: 10. 3969/j. issn. 1000-484X. 2019. 02. 006.

Cui CM, Li YH, Liu Y, et al. Effect of inhibition of immunosuppressive

factor COX-2 on apoptosis of retinal ganglion cells and regulation of p38MAPK signal pathway [J]. Chin J Immunol, 2019, 35 (2) : 156-160. DOI: 10. 3969/j. issn. 1000-484X. 2019. 02. 006.

[20] Li L, Li Y, Miao C, et al. Coriolus versicolor polysaccharides (CVP) regulates neuronal apoptosis in cerebral ischemia-reperfusion injury via the p38MAPK signaling pathway [J/OL]. Ann Transl Med, 2020, 8(18) : 1168 [2021-05-10]. https://pubmed. ncbi. nlm. nih. gov/33241017/. DOI: 10. 21037/atm-20-5759.

[21] Xiong T, Zhang Z, Zheng R, et al. N-acetyl cysteine inhibits lipopolysaccharide-induced apoptosis of human umbilical vein endothelial cells via the p38MAPK signaling pathway [J]. Mol Med Rep, 2019, 20(3) : 2945-2953. DOI: 10. 3892/mmr. 2019. 10526.

[22] 刘高虹, 兰青, 张湾, 等. 西格列汀对高糖诱导的肾小管上皮细胞凋亡和 p38 丝裂原活化蛋白激酶通路的影响 [J]. 中华糖尿病杂志, 2019, 11(4) : 282-286. DOI: 10. 3760/cma. j. issn. 1674-5809. 2019. 04. 011.

Liu GH, Lan Q, Zhang W, et al. Effect of sitagliptin on apoptosis and p38 mitogen activated protein kinase pathway in renal tubular epithelial cells induced by high glucose [J]. Chin J Diabetes Mellitus, 2019, 11(4) : 282-286. DOI: 10. 3760/cma. j. issn. 1674-5809. 2019. 04. 011.

(收稿日期:2021-05-26 修回日期:2021-12-10)

(本文编辑:张宇)

读者 · 作者 · 编者

眼科常用英文缩略语名词解释

AMD: 年龄相关性黄斑变性 (age-related macular degeneration)

ANOVA: 单因素方差分析 (one-way analysis of variance)

BUT: 泪膜破裂时间 (breakup time of tear film)

DR: 糖尿病视网膜病变 (diabetic retinopathy)

EAU: 实验性自身免疫性葡萄膜炎 (experimental autoimmune uveitis)

EGF: 表皮生长因子 (epidermal growth factor)

ELISA: 酶联免疫吸附测定 (enzyme-linked immunosorbent assay)

ERG: 视网膜电图 (electroretinogram)

FFA: 荧光素眼底血管造影 (fundus fluorescein angiography)

FGF: 成纤维细胞生长因子 (fibroblast growth factor)

GFP: 绿色荧光蛋白 (green fluorescent protein)

IFN- γ : γ 干扰素 (interferon- γ)

IL: 白细胞介素 (interleukin)

IOL: 人工晶状体 (intraocular lens)

IRBP: 光间受体视黄类物质结合蛋白 (interphotoreceptor retinoid binding protein)

LASIK: 准分子激光角膜原位磨镶术 (laser in situ keratomileusis)

ICGA: 吲哚菁绿血管造影 (indocyanine green angiography)

LECs: 晶状体上皮细胞 (lens epithelial cells)

miRNA: 微小 RNA (microRNA)

MMP: 基质金属蛋白酶 (matrix metalloproteinase)

mTOR: 哺乳动物类雷帕霉素靶蛋白 (mammalian target of rapamycin)

MTT: 四甲基偶氮唑盐 (methyl thiazolyl tetrazolium)

NF: 核转录因子 (nuclear factor)

OCT: 光相干断层扫描 (optical coherence tomography)

OR: 优势比 (odds ratio)

PACG: 原发性闭角型青光眼 (primary angle-closure glaucoma)

PCR: 聚合酶链式反应 (polymerase chain reaction)

RGCs: 视网膜节细胞 (retinal ganglion cells)

POAG: 原发性开角型青光眼 (primary open angle glaucoma)

RB: 视网膜母细胞瘤 (retinoblastoma)

RPE: 视网膜色素上皮 (retinal pigment epithelium)

RNV: 视网膜新生血管 (retinal neovascularization)

RP: 视网膜色素变性 (retinitis pigmentosa)

S I t: 基础泪液分泌试验 (Schirmer I test)

shRNA: 小发夹 RNA (short hairpin RNA)

siRNA: 小干扰 RNA (small interfering RNA)

α -SMA: α -平滑肌肌动蛋白 (α -smooth muscle actin)

TAO: 甲状腺相关眼病 (thyroid-associated ophthalmopathy)

TGF: 转化生长因子 (transforming growth factor)

TNF: 肿瘤坏死因子 (tumor necrosis factor)

UBM: 超声生物显微镜 (ultrasound biomicroscope)

VEGF: 血管内皮生长因子 (vascular endothelial growth factor)

VEP: 视觉诱发电位 (visual evoked potential)

(本刊编辑部)